Cellular Physiology and Biochemistry

Cell Physiol Biochem 2015;36:2250-2262
DOI: 10.1159/000430189
Published online: July 24, 2015
Accepted: June 12, 2015

1421-9778/15/0366-2250$39.50/0

Original Paper

De Novo Mutation in the SCN5A Gene Associated with Brugada Syndrome

Lumin Wang[a] Xiangyun Meng[b] Zhiguang Yuchi[c] Zhenghang Zhao[d] Dehui Xu[e] David Fedida[f] Zhuren Wang[f] Chen Huang[a,g,h]

[a]Department of Cell Biology and Genetics, School of Basic Medical Sciences, Xi'an Jiaotong University Health Science Center, Xi'an, P.R.China; [b]Department of Cardiovascular Medicine, Xi'an No.1Hospital, Xi'an, P.R.China; [c]Department of Biochemistry and Molecular Biology, University of British Columbia, Vancouver, British Columbia V6T 1Z3, Canada; [d]Department of Pharmacology, Xi'an Jiaotong University Health Science Center, Xi'an, P.R.China; [e]Center for Plasma Biomedicine, Xi'an Jiaotong University, Xi'an, P.R.China; [f]Department of Anesthesiology, Pharmacology and Therapeutics, University of British Columbia, Vancouver, Canada; [g]Key Laboratory of Environment and Genes Related to Diseases, Xi'an Jiaotong University Health Science Center, Xi'an, P.R.China; [h]Cardiovascular Research Center, Xi'an Jiaotong University Health Science Center, Xi'an, P.R.China

Key Words
SCN5A • Sodium Channel Gating • Brugada Syndrome • Arrhythmia • Cardiac depolarization • Ion channel trafficking

Abstract
Background: Brugada syndrome (BrS) is a genetically determined cardiac electrical disorder, characterized by typical electrocardiography (ECG) alterations, and it is an arrhythmogenic syndrome that may lead to sudden cardiac death. The most common genotype found among BrS patients is caused by mutations in the *SCN5A* gene, which lead to a loss of function of the cardiac sodium (Na^+) channel ($Na_v1.5$) by different mechanisms. ***Methods:*** The assay of confocal laser microscopy and western blot were used to identify the expression and location of L812Q at the cell surface. Characterization of Nav1.5 L812Q mutant Na^+ channels was text by patch-clamp recordings, and the PHYRE2 server was used to build a model for human Nav1.5 channel. ***Results:*** Here, we report that a novel missense *SCN5A* mutation, L812Q, localized in the DII-S4 transmembrane region of the $Na_v1.5$ channel protein, was identified in an index patient who showed a typical BrS type-1 ECG phenotype. The mutation was absent in the patient's parents and brother. Heterologous expression of the wild-type (WT) and L812Q mutant $Na_v1.5$ channels in human embryonic kidney cells (HEK293 cells) reveals that the mutation results in a reduction of Na^+ current density as well as ~20 mV hyperpolarizing shift of the voltage dependence of inactivation. The voltage dependence of activation and the time course for recovery from inactivation are not affected by the mutation. The hyperpolarizing shift of the voltage dependence of inactivation caused a reduction of the Na^+ window current as well. In addition, western blot and confocal laser microscopy imaging experiments showed that the

L. Wang and X. Meng contributed equally to this research.

Zhuren Wang, Ph.D.
and Chen Huang, Ph.D.

Department of Anesthesiology, Pharmacology and Therapeutics, 2176 Health Sciences Mall, Vancouver, B.C. V6T 1Z3 (Canada), and and Department of cell Biology and Genetics, School of Basic Medical Sciences, Xi'an Jiaotong University Health Science Center, No.76 West Yanta Road, Xi'an, 710061 Shaanxi (P.R. China)
E-Mail zhuren@mail.ubc.ca, and E-Mail hchen@mail.xjtu.edu.cn

mutation causes fewer channel to be expressed at the membrane than WT channel. A large proportion of the mutant channels are retained in the cytoplasm, probably in the endoplasmic reticulum. ***Conclusion:*** The decrease of channel expression, hyperpolarizing shift of voltage dependence of inactivation, and a decline of Na^+ window current caused by L812Q mutation lead to a reduction of Na^+ current during the upstroke and the repolarization phases of cardiac action potential, which contribute to the development of BrS.

Introduction

Brugada syndrome (BrS) is an autosomal-dominantly inherited cardiac arrhythmogenic syndrome. BrS is characterized by an electrocardiographic (ECG) phenotype consisting of ST-segment elevation in the right precordial leads V1–V3, often referred to as a type-1 BrS pattern, with atypical right bundle branch block; it predisposes to a highly increased risk for syncope and sudden cardiac death (SCD) as a result of polymorphic ventricular tachycardia (VT) or ventricular fibrillation (VF) in the absence of structural heart disease [1-3]. BrS is thought to account for 4% of all SCDs and for up to 20% of unexplained sudden death in patients without cardiac structural disease [4]. However, some patients display a more benign course. The diagnosis of BrS requires the presence of type-1 Brugada ECG phenotype in the right precordial leads (i.e.V1-V3), either spontaneously manifesting or unmasked by sodium channel blockers [5]. Right bundle branch block may be associated with BrS, but it is not a requirement for the diagnosis [1, 6, 7].

Voltage-gated sodium (Na^+) channel $Na_v1.5$ plays a very important role in cardiac impulse propagation. The activation of Na^+ channels is responsible for the generation of the rapid upstroke of the cardiac action potential [8]. Each Na^+ channel is composed of a pore-forming α-subunit and one or more modulating β-subunits [9, 10]. The *SCN5A* gene encodes the α- subunit of $Na_v1.5$ channel, a 2016-amino acid protein. The $Na_v1.5$ α subunit consists of four homologous domains (DI–DIV), each with six transmembrane α helices (S1–S6) linked by intracellular loops [9, 11]. The repeated S1-S4 domains form the channel's voltage sensing domains, primarily mediated by positively charged arginines and lysines positioned at every third residue within each S4 segment [12]. S5, S6 and S5-S6 loops (P-loops) form the functional pore and selectivity filter of Na^+ channel [13]. Mutations in the *SCN5A* gene comprise the most common genotypes found among BrS patients (≈20% of Brugada syndrome patients). Over 300 mutations in the *SCN5A* gene have been identified [3, 14-16]. BrS-associated *SCN5A* mutations cause variable reductions of inward Na^+ current by alterations of channel gating such as delayed activation, enhanced inactivation, slowed recovery from inactivation [17], and/or by impaired trafficking of the channel, the latter reducing expression at cell membrane [18-20]. All of these mechanisms lead to a loss of function of the cardiac Na^+ channel. Decreased inward Na^+ current can affect depolarization and/or repolarization of the cardiac action potential. However, the pathophysiologic mechanism underlying BrS phenotype is still under debate [1].

In the present study, we have screened the *SCN5A* gene from a patient who displayed a characteristic type-1 BrS pattern in ECG. A novel mutation, L812Q, located in the S4 segment of domain II (DII) of the $Na_v1.5$ α-subunit protein has been identified. The functional consequences of L812Q mutation have been examined by measuring the current of the $Na_v1.5$ L812Q mutant channel in a mammalian-cell expression system. We demonstrate that the mutation enhances the Na^+ channel inactivation process and impairs the channel`s expression at the membrane, the probable cause of BrS in the patient.

Materials and Methods

Patient

This study was performed in accordance with the protocol approved by the local ethics committees. Informed consent was obtained from the patient, who was initially presented to the emergency room and

had an ECG examination. A blood sample was obtained from the patient for genotype analysis. After the patient's *SCN5A* mutation was identified, other family members of the patient were invited to participate for the investigation of detailed disease history, ECG examination and blood sample testing.

Genetic analysis

Genomic DNA was purified from peripheral blood lymphocytes using the TiANampBlood DNA kit (TianGen). All exons of *SCN5A* were amplified by polymerase chain reaction (PCR) and sequenced by Bei Jing AuGCT Biotechnology (Sanger sequencing method).

Plasmid constructions

The pEGFP-C1-hH1 plasmid was a gift of Dr. Thomas Zimmer. The cloning of the relevant fragment of *SCN5A* mutation (L812Q) was generated using overlap extension PCR and inserted as an EcoR1/ACC1 fragment into the EcoR1/ACC1 site of *SCN5A* cDNA of pEGFP-C1-hH1. All constructs were purified using Qiagen columns (Qiagen Inc). The cDNA was sequenced to confirm the presence of the correct fragment, containing the mutation.

Cell culture and transient expression in HEK293 cells

HEK293 cells were cultured in Dulbecco modified Eagle's medium (DMEM, PAA Laboratories GmbH, Pasching, Austria) supplemented with 10% fetal bovine serum (FBS, PAA Laboratories GmbH, Pasching, Austria) and 1% penicillin-streptomycin. Cells were maintained at 37°C in a humidified chamber with 95% air and 5% CO_2. To express WT or L812Q mutant $Na_v1.5$ channels, the cells were transiently transfected with plasmids of pEGFP-C1-hH1(WT, 4μg) or pEGFP-C1-hH1-L812Q(4μg) using Lipofectamine 2000 (8μl) transfection reagents (Invitrogen Co., Carlsbad, CA, USA) in 6 well plates. To co-express WT and L812Q mutant channel, equal amounts of pEGFP-C1-hH1 (2μg) and pEGFP-C1-hH1-L812Q (2μg) plasmids (0.5:0.5 ratio) were used to transfect HEK293 cells. The transfected cells were incubated at 37°C for 48 to 72 hours before performing patch-clamp, imaging and biochemical experiments.

Confocal laser microscopy assay

To determine subcellular localization of the WT, WT/ L812Q, and L812Q $Na_v1.5$ channels in HEK293 cells, transfected HEK293 cells were placed on poly-D-lysine-coated cover slips. The cells were fixed with 4% formaldehyde for 20 minutes, and then incubated with 0.5% Triton X-100. After washed three times with PBS, the cells were incubated with a goat anti-mouse antibody (Millipore), and measured by confocal laser microscopy (Leica).

Immunofluorescence microscopy

To determine the effect of L812Q on location of Nav1.5, we also performed immunofluorescence staining using the Na/K-ATPase (Abcam), SCN5A (Abcam) and Calnexin (Abcam 1:100) anti-body. After 48h, the transfected L812Q cell lines were fixed with 4% formaldehyde for 20 minutes, then incubated with 0.5% Triton X-100. Rabbit/mouse anti- Na/K-ATPase/ SCN5A/ Calnexin antibody was used for immunofluorescence staining. After washed three times with PBS, the cells were incubated with a goat anti-rabbit/mouse antibody (Millipore) and measured by immunofluorescence microscopy.

Biotinylation of cell surface proteins

Cell surface proteins of HEK293 cells transfected with WT, WT/L812Q, L812Q were isolated using the Pierce Cell Surface Protein Isolation kit (Thermo Scientific) following manufacturer's instructions. Briefly, sulfo-NHS-biotin solution was prepared by dissolving one vial of sulfo-NHS-biotin into 48 ml of ice cold PBS. Then, cells at 90–95% confluence in a 10-cm dish were incubated with 10 ml of sulfo-NHS-biotin solution for 30 min at 4°C. After the reaction was quenched by 500 μl of quenching solution, cells were scraped and washed with TBS buffer to remove extra biotin solution. After centrifugation to remove supernatant, cell pellets were lysed in lysis buffer by sonication and clarified by centrifugation. Clear supernatant was reacted with immobilized NeutrAvidin gel slurry in columns (Pierce) to isolate surface proteins. Columns were washed and protein eluted in sample buffer containing DTT. Surface proteins were resolved on a SDS-PAGE gel and the samples were analyzed by western blot.

Western blots

Transfected HEK293cells were placed on six-well plates, total proteins were extracted using RIPA buffer, supplemented with protease inhibitor (invitrogen). Protein concentration was estimated by quantitative analyzer (GeneQuant pro RNA/DNA). Protein was then separated with an 8% to 10% SDS-PAGE (Invitrogen), transferred to a nitrocellulose membrane, then incubated with the *SCN5A*, Na/K-ATPase or β-ACTIN antibodies (Abcam). After washing three times with TBST, the membrane was incubated with a goat anti-mouse antibody (Bioworld). For the total proteins, relative protein expression was normalized to β-ACTIN, and for the transmembrane proteins, relative protein expression was then normalized to Na/K-ATPase levels.

Patch-clamp recordings

Whole-cell patch-clamp recording [21] was performed at room temperature (21–24°C) with an Axopatch 200B amplifier (Axon Instruments, Foster City, CA, USA). The extracellular solution contained (in mM): NaCl 140, CsCl 10, $CaCl_2$ 2, $MgCl_2$ 1, glucose 5, and HEPES 10, pH 7.4 with NaOH. Electrodes had resistances of 1 – 2 MΩ when filled with the filling solution containing (in mM): CsCl 110, NaCl 10, EGTA 11, $MgCl_2$ 1 and HEPES 10, pH 7.2 with CsOH. Measured series resistance was between 1 and 3 MΩ for all recordings, and was compensated by ≈80%. When the series resistance changed during the course of an experiment, data were discarded. The membrane potential was not corrected for a small liquid junction potential (~ 6.7 mV). pClamp6 software (Axon Instruments, Foster City, CA, USA) was used for the experiments and data analysis. $Na_v1.5$ current (I_{Na}) densities (pA/pF) were obtained by dividing the peak I_{Na} by the cell capacitance read from the Axopatch 200B amplifier. Na^+ currents were elicited by 10 mV depolarizing steps between -80 to +60 mV from a holding potential of -120 mV. The pulse duration was 40 ms with an interval of 2 s. The plots of steady-state activation and inactivation were fitted by Boltzmann equation: $y=1/ [1+\exp(V-V_{0.5})/k]$, where $V_{0.5}$ is the voltage at which sodium channels are half-maximally activated, and k was the slope factor. The recovery from inactivation at -120 mV was fitted by a bi-exponential equation: $y=y0+Af[1-\exp(-t/\tau f)]+As[1-\exp(-t/\tau s)]$, where Af is the fraction of fast components, As is the fraction of slow components, τf is time constants of fast components of recovery and current Decay, τs is the time constants of slow components of recovery and current decay. To obtain the voltage-dependence of activation and inactivation, all data were recorded after establishing the whole-cell configuration for 5 minutes.

Homologous model for human $Na_v1.5$ channel

PHYRE2 server [22] was used to build a model for human $Na_v1.5$ channel, based on the structure of a bacterial voltage-gated sodium channel (NavAb) [23]. The four α subunits were modeled individually and superposed on the NavAb structure. Chimera [24] was used to minimize the tetrameric models for WT and mutant $Na_v1.5$ channel.

Statistical analysis

Results are presented as means ± standard errors of the mean (SEM). Where indicated, a *t*-test was performed by using SPSS13.0 software (SPSS, Chicago, IL, USA). A p value less than 0.05 was considered statistically significant.

Results

Clinical studies

The patient, a 58-year-old man of Chinese ancestry, presented to the emergency room with the onset of chest distress and agonal respiration, following with vomiting, choking and violent pain on ventri- thighs of both lower extremities. The patient had a 15 year history of transit occurrence of paroxysmal chest pain and stuffiness. The ECG was characteristic of spontaneous type-1 BrS, displaying a prominent ST-segment elevation in the right precordial leads, V1–V2, associated with the presence of incomplete right bundle branch block (Fig. 1). The ECG showed that the patient remained in sinus rhythm, with a heart rate of about 83 beats a minute; prolongation of QT interval, entricular polymorphic tachycardia or fibrillation were not observed. The patient had never experienced syncope, amaurosis and

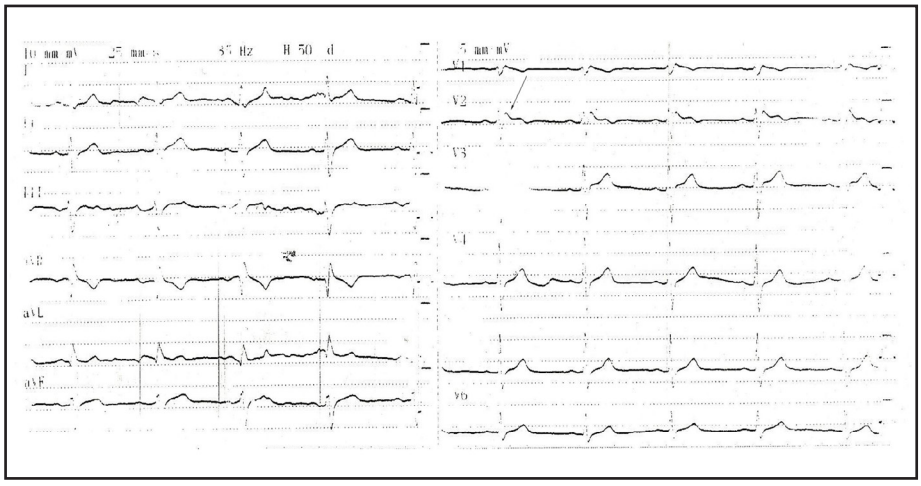

Fig. 1. Electrocardiogram (ECG) recordings of the index patient in precordial leads V1-V6. Note the marked ST-segment elevation in the leads V1–V2. The patient remained in sinus rhythm.

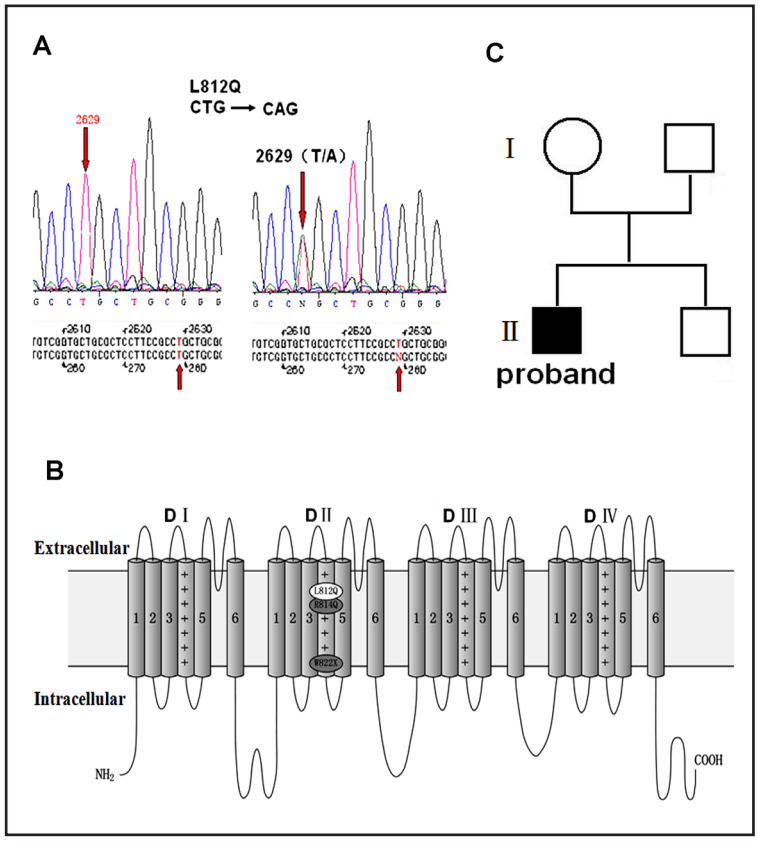

Fig. 2. Genetic analysis of the index patient with the *SCN5A* mutation. (A) Sequence analysis of the *SCN5A* gene reveals a heterozygous missense mutation in exon 16, resulting in a change of Leucine (L) to Glutamine (Q) at position 812. (B) Membrane topology of $Na_v1.5$ channel protein. The location of the identified L812Q mutation is shown. (C) Family pedigree. The filled black square indicates the carrier of the L812Q mutation.

disturbance of consciousness. No abnormal observation was found with an echocardiogram and chest X-ray. The patient had no concomitant risks such as diabetes, hypertension, or thromboembolic disease. The investigation of the patient's family history found no other case of BrS, sustained ventricular arrhythmias, or sudden death. The patient was diagnosed with BrS according to the type-1 BrS pattern in ECG and the clinical symptoms [25].

Mutational analysis

The *SCN5A* gene associated with BrS was screened in the present study. A novel heterozygous missense mutation in *SCN5A* gene was identified in the patient by PCR followed by DNA sequencing (Fig. 2A). There was a heterozygous T to A base change at position 2629 in exon 16, which presumably changed the coding from a leucine (L) (CTG) to a glutamine

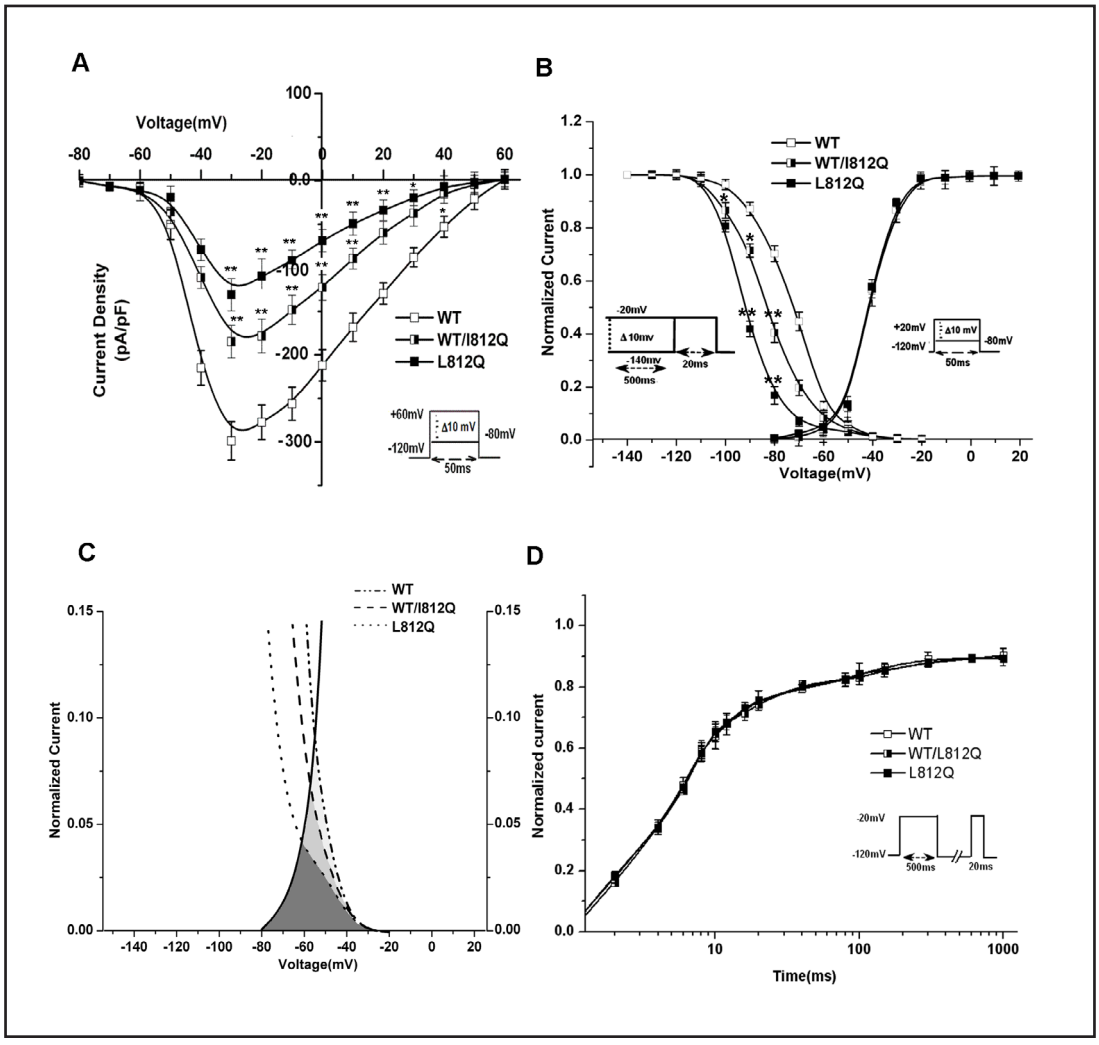

Fig. 3. Comparison of the electrophysiological characteristics of WT and L812Q mutant $Na_v1.5$ channels. WT, L812Q mutant or both WT and L812Q mutant (WT/L812Q) channels were transiently expressed in HEK-293 cells. Co-expression of WT and L812Q mutant channels (WT/L812Q) was conducted as described in METHODS. (A) Na^+ current density and voltage relationships obtained from the cells expressing WT, L812Q or WT/L812Q channels. The Na^+ currents were measured at membrane potentials between -80 to +60 mV. The holding potential was -120 mV. The experimental pulse protocol was illustrated in the inset. (B) Steady-state activation and inactivation curves for WT, L812Q or WT/L812Q channels. The insets illustrate the protocols for the measurement of steady-state activation and inactivation. The parameters for fitting the curves are seen in RESULTS and Table 1. (C) The change of the Na^+ window currents induced by $Na_v1.5$ L812Q mutant channel. Overlap of steady-state inactivation curves and activation curves display the window currents of WT, L812Q and WT/L812Q channels. (D) The time course of recovery from inactivation for WT, L812Q and WT/L812Q channels. The curves are fitted using bi-exponential function. The time constants are seen in RESULTS and Table 1. The inset shows the pulse protocol used for the measurement of recovery from inactivation.

(Q) (CAG) at position 812, that was, from a hydrophobic amino acid of non-polarity to a hydrophilic amino acid of polarity. The L812Q mutation was located in the S4 segment of domain II (DII) of the $Na_v1.5$ α-subunit protein (Fig. 2B). This mutation had not been registered in the SNP database of the National Center for Biotechnology Information (*www.ncbi.nlm.nih.gov*). No other mutation was found in the gene screen. The patient's parents and brother were all negative for the L812Q mutation (Fig. 2C).

Table 1. Gating kinetics of WT and L812Q. The numbers in the parentheses represent number of patches. Af = the fraction of fast components; As = the fraction of slow components; k = slope factor; τf = time constants of fast components of recovery and current decay; τs = the time constants of slow components of recovery and current decay; V1/2 = the membrane potential for half maximal activation or inactivation; WT = wild type. **= P<0.01

	WT	WT/L812Q	L812Q
Steady- state activation			
V1/2(mV)	-40.91±0.21(9)	-41.06±0.33(8)	-41.24±0.22(7)
K(mV)	5.10±0.34(9)	4.97±0.30(8)	4.72±0.21(7)
Steady-state inactivation			
V1/2(mV)	-72.70±0.94(7)	-83.50±0.35(8)**	-92.40±0.63(8)**
K(mV)	8.00±0.83(7)	8.39±0.31(8)	6.20±0.43(8)*
Recover from inactivation			
τfast (ms)	5.29±0.17(8)	5.05±0.26(8)	5.16±0.26(8)
τslow (ms)	109.44±20.04(8)	109.47±28.17(8)	110.48±29.06(8)
Afast	0.86±0.02(8)	0.90±0.02(8)	0.89±0.02(8)
Aslow	0.15±0.01(8)	0.14±0.02(8)	0.14±0.02(8)

Characterization of $Na_v1.5$ L812Q mutant Na^+ channels

In order to understand the pathophysiologic mechanisms underlying the BrS phenotype in the patient, $Na_v1.5$ channels were transiently expressed in HEK 293 cells and the effect of the L812Q mutation on channel function was investigated by whole-cell patch clamp recordings. The L812Q mutation significantly affected the function of the $Na_v1.5$ channel. Compared to WT $Na_v1.5$ channel, the L812Q mutation greatly reduced the Na^+ current amplitude. The averaged current-voltage relations plotted in Fig. 3A showed that the current density was drastically decreased by L812Q mutation. The maximum peak Na^+ current density at -30 mV were 298 ± 18 pA/pF (n = 8) and 130 ± 24 pA/pF (n = 9) for $Na_v1.5$ WT and L812Q mutant channel, respectively. However, the voltages for the threshold of activation and the maximum peak current as well as the reversal potential for the current were not significantly altered by the L812Q mutation. The voltage dependence of steady-state activation and inactivation for $Na_v1.5$ WT and L812Q mutant channel were determined as shown in Fig. 3B. The activation curves were not significantly different between WT and L812Q mutant channels, with a half-activation voltage ($V_{0.5}$) of -40.9 ± 0.2 mV and a slope factor (k) of 5.1 ± 0.3 mV for the $Na_v1.5$ WT channel (n = 9) and a $V_{0.5}$ of -41.2 ± 0.2 mV and a k of 4.7 ± 0.2 mV for the L812Q mutant channel (n = 7). In contrast to the activation curves, the steady-state inactivation curve was significantly negatively shifted by the L812Q mutation. For the $Na_v1.5$ WT channel, the $V_{0.5}$ and k for the steady-state inactivation curve were -72.7 ± 0.9 mV and 8.0 ± 0.8 mV (n = 8), respectively. For the L812Q mutant channel, the $V_{0.5}$ was shifted to -92.4 ± 0.6 mV with a k of 6.2 ± 0.4 mV (n = 7). These results indicated about 20 mV hyperpolarizing shift of the inactivation curve by L812Q mutation, suggesting that L812Q mutation enhanced the channel inactivation. Furthermore, the hyperpolarizing shift of voltage dependence of inactivation reduced the Na^+ window current as shown in Fig. 3C. The Na^+ window current was estimated from the overlay of activation and inactivation curves [26]. The negative shift of steady-state inactivation curve with an unchanged activation curve significantly decreased the Na^+ window current. The peak of window current occurred at -61.5 ± 0.5 mV (n=8) and -52.2 ± 0.8 mV (n=8) for L812Q and WT channel, respectively, indicating a more negative voltage range for the window current in the L812Q mutant than in the WT channel. The kinetics of recovery from inactivation was also measured. The fast and slow time constant for recovery from inactivation were 5.16 ± 0.26 and 110.48 ± 29.06 ms (n = 8), respectively, for L812Q mutant channel, not significantly different from that for the $Na_v1.5$ WT channels (5.29 ± 0.17 and 109.44 ± 20.04 ms, n=8) (Fig. 3D) (Table 1), suggesting that the conformation of the inactivated channel protein might not be altered by the L812Q mutation. Thus, the observed hyperpolarizing shift of the voltage dependence of inactivation and reduction of Na^+ window current would result in a decrease

in the numbers of open $Na_v1.5$ channels during the upstroke and the repolarization phases of the cardiac action potential, leading to a decrease of the inward depolarizing Na^+ current.

Consistent with an autosomal dominant trait, the proband was found to be heterozygous

In order to understand the heterozygous state of $Na_v1.5$ channel in the patient, WT and L812Q mutant $Na_v1.5$ channels were co-expressed in HEK293 cells (WT/L812Q). Na^+ currents recorded from the cells co-expressing WT and L812Q mutant channel mimicking the heterozygous condition appeared to be a mixture of the mutant and WT channel. The Na^+ current density was less reduced by WT/L812Q co-expression (Fig. 3A). The maximum peak Na^+ current density at -30 mV was 184 ± 19 pa/pF (n = 9) for WT/L812Q channels, in between WT and L812Q mutant channels (Fig. 3A). The steady-state activation curve for WT/L812Q overlapped with that for WT and L812Q mutant channels, with a $V_{0.5}$ of -41.1 ± 0.3 mV and a *k* of 5.0 ± 0.3 mV (n = 8) (Fig. 3B) (Table 1). The steady-state inactivation curve was still negatively shifted, but to a lesser extent than the L812Q mutant channel, with a $V_{0.5}$ of -83.5 ± 0.4 mV and a *k* of 8.4 ± 0.3 mV for the WT/L812Q channel co-expression (n = 8) (Fig. 3B) (Table 1). Consequently, the Na^+ window current was increased to an extent between the WT and L812Q mutant channels (Fig. 3C). The time course of recovery from inactivation was not altered by WT/L812Q co-expression, overlapping with that for WT and L812Q mutant channels (Fig. 3D) (Table 1). These results suggested that at the heterozygous state, the L812Q mutation did not exert a dominant-negative effect on WT channels.

Impaired trafficking of $Na_v1.5$ channel caused by L812Q mutation

Because the L812Q mutation greatly reduced Na^+ current density, we further investigated the effect of the L812Q mutation on the trafficking of the channel to the plasma membrane. The top panel of Fig. 4A showed typical images for the subcellular localization of the WT $Na_v1.5$ and L812Q channels. In agreement with the reduced Na^+ current density, the surface expression of the L812Q mutant channels was decreased, compared to that of WT $Na_v1.5$ channels. Co-expression of WT and L812Q mutant $Na_v1.5$ channels also showed lowered membrane associated fluorescence and increased intracellular fluorescence compared to the WT $Na_v1.5$ channels. Next, we used the assay of immunofluorescence to observe the co-localization of L812Q with Na/K-ATPase, or the co-localization of L812Q with calnexin (bottom panel of Fig. 4A). The results showed that more intracellular retention was associated with L812Q mutant channels.

Western blot assay was used to further evaluate the amount of WT and L812Q mutant $Na_v1.5$ channels proteins at the total cell or cell surface. Fig. 4 showed that the expression of L812Q mutant channel at the plasma membrane surface was significantly decreased compared to that of WT $Na_v1.5$ channels and total cell expression of the L812Q mutant was reduced compared to WT channels. The co-expressed WT/L812Q channel also showed decreased expression at the plasma membrane compared to homozygous WT $Na_v1.5$ channels. Taken together, the results indicated that the L812Q mutation led to increased intracellular retention of the channel, reducing the expression at the plasma membrane surface.

Discussion

BrS is an inherited cardiac disorder with ECG characteristics of ST-segment elevation in the right precordial leads V1–V3 and right bundle branch block [2]. BrS accounts for ≥20% of sudden cardiac death in patients with structurally normal hearts and ≥4% of all sudden deaths [27, 28]. Many researches show that a lot of genes are involved in development of BrS, such as *SCN5A, GPD1L, CACNA1C, CACNB2, SCN1B, KCNE3, SCN3B*. Mutations in the *SCN5A* gene encoding cardiac $Na_v1.5$ channel have been identified that account for ≈20% to 30% of all BrS cases, 11-12% can be attributed to mutations in *CACNA1C* and *CACNB2*. Minor contributions to BrS cases are made from mutations in other genes [19, 29]. Here, we report

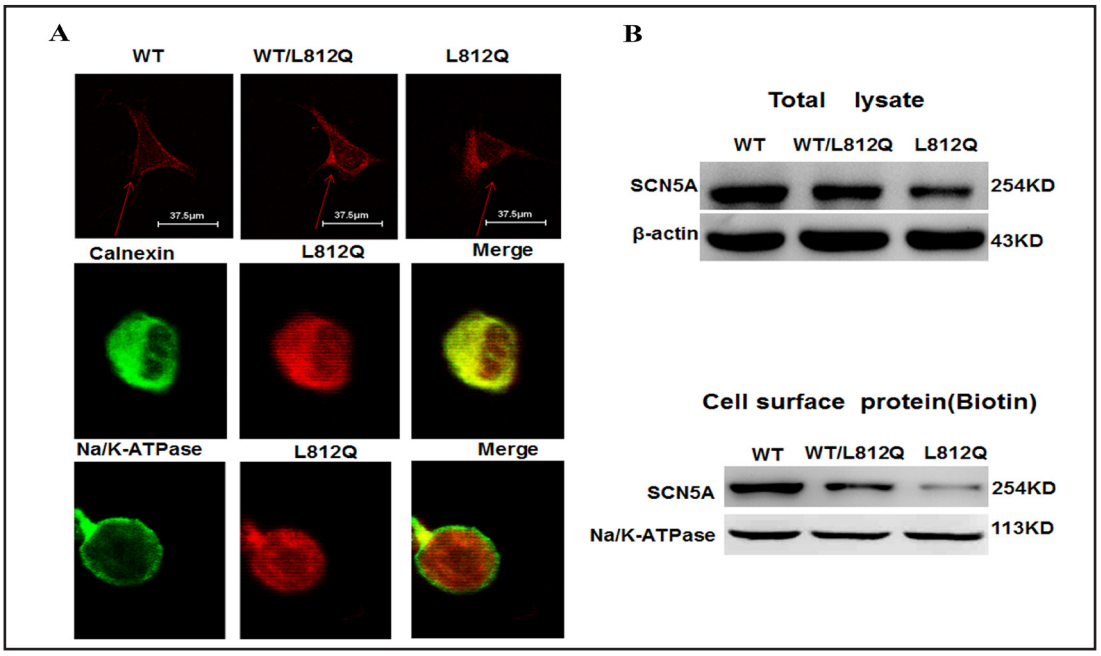

Fig. 4. Location of WT and L812Q mutant $Na_v1.5$ channels expressed in HEK293 cells. (A) Top panel: Confocal microscopy images of the cells transiently expressing the channels as indicated in the figure. Note that the clear plasma membrane localization of the WT $Na_v1.5$ channels is reduced with WT/L812Q co-expression and not observable with only expression of L812Q mutant channels. Scale bar indicates 37.5 μm. Bottom panel: immunofluorescence images of the cells transiently expressing the L812Q channels. The green stain is presented Na/K-APTase and calnexin respectively, the red stain is presented SCN5A-L81Q. (B) Western blot of lysates of HEK293 cells transiently transfected with WT, L812Q, or WT/L812Q channel. Top panel: the expression of WT, L812Q, or WT/L812Q channel on total proteins, β-actin are used as a control. The bottom panel: the expression of WT, L812Q, or WT/L812Q channel on transmembrane proteins, Na/K-ATPase as a control (n=5).

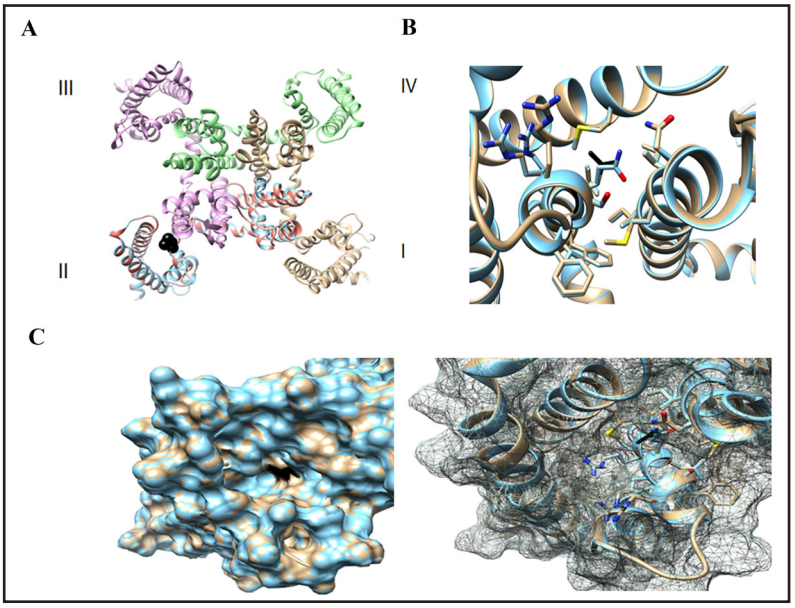

Fig. 5. Mapping of L812Q residue onto a $Na_v1.5$ homology model. (A) Top view of $Na_v1.5$ structural model. The model is created by Phyre2 server [22] based on the crystal structure of NavAb (PDB:3RVZ) and energy minimized by chimera. Wild type Domains I through IV are colored in gold, cyan, purple and green, respectively. Domain II with L812Q mutation is colored in red. Leu812 is shown as black spheres. (B) Enlarged view of the local environment of L812Q. The side chains of residue 812 (shown in black) and the neighboring residues are displayed as stick representations (wild type in gold and mutant in cyan). (C) Surface view of L812Q. Residue 812 (black) is half buried and half exposed to a water cavity (wild type in gold and mutant in cyan).

a novel mutation in the cardiac $Na_v1.5$ channel, L812Q, in a proband with BrS. This missense mutation is in the DII-S4 transmembrane helices of $Na_v1.5$ channel. Unlike most individuals diagnosed with BrS who have inherited the pathogenic variant from a parent, the proband has no family record of BrS. Sequencing of the DNA failed to identify the mutation in his parents and brother, indicating that this L812Q mutation is likely de novo. BrS caused by de novo mutation is rare, estimated at about 1% of all cases with the syndrome[30].

The human sodium channel $Na_v1.5$, encoded by SCN5A gene, plays a critical role in cardiac excitability and the propagation of action potentials [31]. Mutations in the SCN5A gene can cause a number of inherited arrhythmia syndroms [32]. In our research, we have investigated the functional consequences of the L812Q mutation on the biophysical properties of $Na_v1.5$ channel. Channels with the L812Q mutation exhibited severely reduced, by ~60%, peak Na^+ current density (Fig 3A). In addition, the mutation resulted in a negative shift of the steady-state inactivation curve of the Na^+ current by ~20 mV without change of the voltage dependence of activation (Fig. 3B). Such a shift represents a decreased availability and an enhanced stabilization of the inactivated state of the Na^+ channels, causing decrease of Na^+ current during activation and the window Na^+ current during the course of repolarization. Consequently, the reduction of the Na^+ current during the depolarization and the repolarization phases of the action potential are likely to decrease action potential upstroke velocity, leading to slow atrial and ventricular conduction and disrupt the balance between the inward and outward currents during phase 1 of the action potential, likely shortening the plateau phase of the action potential. The effects of L812Q mutation on the function of $Na_v1.5$ channel further proved that loss of function of Na^+ channel can cause BrS.

To mimic the hyterozygous *in vivo* situation wherein the WT and mutated alleles co-exist in the same patient, we performed co-expression experiments in which equal amounts of WT and L812Q mutation DNA were used to transfect HEK cells. We found that the density of Na^+ currrent was reduced to ~60% of the WT Na^+ current density, and the voltage dependence of inactivation was also shifted towards negative voltages compared to the WT channel. Some research showed that when co-expressing trafficking-deficient BrS *SCN5A* mutations with WT $Na_v1.5$ channel (0.5:0.5 in ratio) in heterologous expression systems, it is observed that the Na^+ current was reduced by about 50% compared to the Na^+ current produced by expressing only WT $Na_v1.5$ channel [33-35]. Such reduction of Na^+ current is due to the haploinsufficiency of WT $Na_v1.5$ channel. However, other research showed that co-expressing mutations with WT channel, the Na^+ current density was also drastically reduced by more than 40% compared to the control condition where 100% of WT channels were expressed, suggesting that those mutations exert a dominant negative effect on WT channels [36, 37]. Furthermore, a recent study report that some BrS *SCN5A* mutations heterologously in the homozygous state, only minor biophysical defects, but not produce a BrS phenotype. However, when these mutations were co-expressed with WT $Na_v1.5$ channel in patients, these atypical mutations could lead to a severe reduction in Na^+ current densities similar to typical BrS mutations, i.e., they appear to exert a dominant-negative effect. This decrease in current density was the result of reduced surface expression of both mutant and WT channels [38]. Unlike the mutations that exert dominant negative effects on WT channels, the effect of L812Q mutation on channel function was less severe as the channel still induced significant Na^+ current in a heterologous expression system in the homozygous state. Co-expression of the L812Q mutation with WT $Na_v1.5$ channel decreased Na^+ current density by about 40% (Fig. 3). The relatively benign reduction of the Na^+ current induced by co-expression of L812Q mutation and WT channel is consistent with haploinsufficiency without producing dominant negative effect, suggesting that L812Q mutation did not exert a dominant-negative effect on WT channels. Interestingly, when we text the expression of L812Q channel protein on total proteins by using western blot, we found that the expression of L812Q was lesser than that of WT channel (Fig. 4), suggesting that some proteins might be degraded in cytoplasm caused by intracellular retention of L812Q channel protein.

L812Q occurs in the DII–S4 transmembrane helices of the $Na_v1.5$ channel protein, which is one of the "voltage sensors" that carries a number of positively charged residues,

lysine and arginine, to sense the changes in the transmembrane electrical field for activation gating of the channel [39]. Other mutations affecting residues in the DII-S4 (R808P, R811H, L812P, R814Q, and W822X) have been reported to be associated with BrS [40]. The functional consequences of these mutations include impairment of the channel trafficking and alterations of the channel gating process. Similar to these mutations, L812Q mutation has the same function (Fig. 3 and 4). The recent determined structures of bacterial sodium channels gave us good templates to model the mutations in their human relatives. The homologous models of wild type and mutant $Na_v1.5$ (Fig. 5), generated based on the NavAb crystal structure [23], indicate that the L812Q mutation probably does not change the overall structure of the channel (overall RMS 0.096A between 11446 atom pairs). L812 is located in a hydrophobic pocket formed by S1/S4 from domain II and S5 from domain III. The hydrophobic properties of the pocket (M734, L813, V815, I1346, I1349, M1350), is conserved in NavAb as well as many other Na_v channels, suggesting a probable functional importance of these interactions. Introduction of a hydrophilic bulky residue glutamine in the hydrophobic pocket will no doubt destabilize the interface between S4 from domain II and S5 from domain III, and affect the relevant motion. From the surface view, L812 is half buried and half exposed to a water cavity connected to the extracellular side, suggesting a function, perhaps, like a lid for the hydrophobic pocket. Mutations to glutamine will open the lid and introduce water molecules further into the crevice between S4 and S5, which may lower the energy barrier even more to facilitate the relative motion between two helices. The possible effect of L812Q mutation on the interaction between DII-S4 and DIII-S5 of the channel are very intriguing. Whether these interactions will affect the inactivation process of the Na_v channel is highly worthy of further exploration in the future studies.

In summary, we have identified a $Na_v1.5$ mutation, L812Q, located in the DII-S4 transmembrane region, in a BrS patient. This novel mutation not only causes a reduction of channel expression at the cell surface, but also reduces the Na^+ current and significantly hyperpolarizes the voltage-dependent inactivation of the channels. Those biophysical modifications of Nav1.5 by L821Q predispose to the BrS of this patient. However, we find that L812Q is de novo mutation and does not exert a dominant-negative effect on WT channels, suggesting that the environmental factor, other genes or some hidden reasons may be involved in pathogenicity of the L812Q and those clinical features. Further studies are needed to answer these questions. Additionally, in the context of the recently published crystal structure of the bacterial NavAb channels, the evident functional effects of the mutation correlate with a lack of change of the overall structure, suggesting that the disruption of specific intra- and/or inter-domain interaction could underlie the mutation-dependent effects.

Acknowledgments

We thank Dr. David Steele for valuable comments on the manuscript. National Natural Science Foundation of China -Canada Cooperation Projects (81161120549).

Disclosure Statement

No potential conflicts of interest were disclosed.

References

1 Berne P, Brugada J: Brugada syndrome 2012. Circ J 2012;76:1563-1571.
2 Brugada P, Brugada J: Right bundle branch block, persistent ST segment elevation and sudden cardiac death: a distinct clinical and electrocardiographic syndrome. A multicenter report. J Am Coll Cardiol 1992;20:1391-1396.

3 Antzelevitch C, Brugada P, Brugada J, Brugada R, Shimizu W, Gussak I, Perez Riera AR: Brugada syndrome: a decade of progress. Circ Res 2002;91:1114-1118.
4 Antzelevitch C, Brugada P, Borggrefe M, Brugada J, Brugada R, Corrado D, Gussak I, LeMarec H, Nademanee K, Perez Riera AR, Shimizu W, Schulze-Bahr E, Tan H, Wilde A: Brugada syndrome: report of the second consensus conference: endorsed by the Heart Rhythm Society and the European Heart Rhythm Association. Circulation 2005;111:659-670.
5 Miyazaki T, Mitamura H, Miyoshi S, Soejima K, Aizawa Y, Ogawa S: Autonomic and antiarrhythmic drug modulation of ST segment elevation in patients with Brugada syndrome. J Am Coll Cardiol 1996;27:1061-1070.
6 Gussak I, Antzelevitch C, Bjerregaard P, Towbin JA, Chaitman BR: The Brugada syndrome: clinical, electrophysiologic and genetic aspects. J Am Coll Cardiol 1999;33:5-15.
7 Kasanuki H, Ohnishi S, Ohtuka M, Matsuda N, Nirei T, Isogai R, Shoda M, Toyoshima Y, Hosoda S: Idiopathic ventricular fibrillation induced with vagal activity in patients without obvious heart disease. Circulation 1997;95:2277-2285.
8 Balser JR: Structure and function of the cardiac sodium channels. Cardiovasc Res 1999;42:327-338.
9 Gellens ME, George AL, Jr., Chen LQ, Chahine M, Horn R, Barchi RL, Kallen RG: Primary structure and functional expression of the human cardiac tetrodotoxin-insensitive voltage-dependent sodium channel. Proc Natl Acad Sci U S A 1992;89:554-558.
10 Makita N, Bennett PB, George AL, Jr: Molecular determinants of beta 1 subunit-induced gating modulation in voltage-dependent Na^+ channels. J Neurosci 1996;16:7117-7127.
11 Noda M: Structure and function of sodium channels. Ann N Y Acad Sci 1993;707:20-37.
12 Jensen MO, Jensen TR, Kjaer K, Bjornholm T, Mouritsen OG, Peters GH: Orientation and conformation of a lipase at an interface studied by molecular dynamics simulations. Biophys J 2002;83:98-111.
13 Terlau H, Heinemann SH, Stuhmer W, Pusch M, Conti F, Imoto K, Numa S: Mapping the site of block by tetrodotoxin and saxitoxin of sodium channel II. FEBS Lett 1991;293:93-96.
14 Priori SG, Napolitano C, Giordano U, Collisani G, Memmi M: Brugada syndrome and sudden cardiac death in children. Lancet 2000;355:808-809.
15 Kapplinger JD, Tester DJ, Alders M, Benito B, Berthet M, Brugada J, Brugada P, Fressart V, Guerchicoff A, Harris-Kerr C, Kamakura S, Kyndt F, Koopmann TT, Miyamoto Y, Pfeiffer R, Pollevick GD, Probst V, Zumhagen S, Vatta M, Towbin JA, Shimizu W, Schulze-Bahr E, Antzelevitch C, Salisbury BA, Guicheney P, Wilde AA, Brugada R, Schott JJ, Ackerman MJ: An international compendium of mutations in the SCN5A-encoded cardiac sodium channel in patients referred for Brugada syndrome genetic testing. Heart Rhythm 2010;7:33-46.
16 Li A, Saba MM, Behr ER: Genetic biomarkers in Brugada syndrome. Biomark Med 2013;7:535-546.
17 Makiyama T, Akao M, Haruna Y, Tsuji K, Doi T, Ohno S, Nishio Y, Kita T, Horie M: Mutation analysis of the glycerol-3 phosphate dehydrogenase-1 like (GPD1L) gene in Japanese patients with Brugada syndrome. Circ J 2008;72:1705-1706.
18 Kattygnarath D, Maugenre S, Neyroud N, Balse E, Ichai C, Denjoy I, Dilanian G, Martins RP, Fressart V, Berthet M, Schott JJ, Leenhardt A, Probst V, Le Marec H, Hainque B, Coulombe A, Hatem SN, Guicheney P: MOG1: a new susceptibility gene for Brugada syndrome. Circ Cardiovasc Genet 2011;4:261-268.
19 Chen Q, Kirsch GE, Zhang D, Brugada R, Brugada J, Brugada P, Potenza D, Moya A, Borggrefe M, Breithardt G, Ortiz-Lopez R, Wang Z, Antzelevitch C, O'Brien RE, Schulze-Bahr E, Keating MT, Towbin JA, Wang Q: Genetic basis and molecular mechanism for idiopathic ventricular fibrillation. Nature 1998;392:293-296.
20 Tan HL, Bezzina CR, Smits JP, Verkerk AO, Wilde AA: Genetic control of sodium channel function. Cardiovasc Res 2003;57:961-973.
21 Hamill OP, Marty A, Neher E, Sakmann B, Sigworth FJ: Improved patch-clamp techniques for high-resolution current recording from cells and cell-free membrane patches. Pflugers Arch 1981;391:85-100.
22 Kelley LA, Sternberg MJ: Protein structure prediction on the Web: a case study using the Phyre server. Nat Protoc 2009;4:363-371.
23 Payandeh J, Scheuer T, Zheng N, Catterall WA: The crystal structure of a voltage-gated sodium channel. Nature 2011;475:353-358.
24 Pettersen EF, Goddard TD, Huang CC, Couch GS, Greenblatt DM, Meng EC, Ferrin TE: UCSF Chimera--a visualization system for exploratory research and analysis. J Comput Chem 2004;25:1605-1612.

25 Wilde AA, Antzelevitch C, Borggrefe M, Brugada J, Brugada R, Brugada P, Corrado D, Hauer RN, Kass RS, Nademanee K, Priori SG, Towbin JA: Proposed diagnostic criteria for the Brugada syndrome: consensus report. Circulation 2002;106:2514-2519.
26 Gilly WF, Armstrong CM: Threshold channels--a novel type of sodium channel in squid giant axon. Nature 1984;309:448-450.
27 Benito B, Brugada J, Brugada R, Brugada P: Brugada syndrome. Rev Esp Cardiol 2009;62:1297-1315.
28 Antzelevitch C, Brugada P, Borggrefe M, Brugada J, Brugada R, Corrado D, Gussak I, LeMarec H, Nademanee K, Perez Riera AR, Shimizu W, Schulze-Bahr E, Tan H, Wilde A: Brugada syndrome: report of the second consensus conference. Heart Rhythm 2005;2:429-440.
29 Veerakul G, Nademanee K: Brugada syndrome: two decades of progress. Circ J 2012;76:2713-2722.
30 Brugada R, Campuzano O, Brugada P, Brugada J, Hong K: Brugada Syndrome; in Pagon RA, Adam MP, Ardinger HH, Bird TD, Dolan CR, Fong CT, Smith RJH, Stephens K, (eds): GeneReviews. Seattle (WA), University of Washington, Seattle, 1993.
31 Remme CA: Cardiac sodium channelopathy associated with SCN5A mutations: electrophysiological, molecular and genetic aspects. J Physiol 2013;591:4099-4116.
32 Zimmer T, Surber R: SCN5A channelopathies--an update on mutations and mechanisms. Prog Biophys Mol Biol 2008;98:120-136.
33 Dolz-Gaiton P, Nunez M, Nunez L, Barana A, Amoros I, Matamoros M, Perez-Hernandez M, Gonzalez de la Fuente M, Alvarez-Lopez M, Macias-Ruiz R, Tercedor-Sanchez L, Jimenez-Jaimez J, Delpon E1, Caballero R1, Tamargo J: Functional characterization of a novel frameshift mutation in the C-terminus of the Nav1.5 channel underlying a Brugada syndrome with variable expression in a Spanish family. PLoS One 2013;8:e81493.
34 Calloe K, Refaat MM, Grubb S, Wojciak J, Campagna J, Thomsen NM, Nussbaum RL, Scheinman MM, Schmitt N: Characterization and mechanisms of action of novel NaV1.5 channel mutations associated with Brugada syndrome. Circ Arrhythm Electrophysiol 2013;6:177-184.
35 Keller DI, Barrane FZ, Gouas L, Martin J, Pilote S, Suarez V, Osswald S, Brink M, Guicheney P, Schwick N, Chahine M: A novel nonsense mutation in the SCN5A gene leads to Brugada syndrome and a silent gene mutation carrier state. Can J Cardiol 2005;21:925-931.
36 Keller DI, Rougier JS, Kucera JP, Benammar N, Fressart V, Guicheney P, Madle A, Fromer M, Schlapfer J, Abriel H: Brugada syndrome and fever: genetic and molecular characterization of patients carrying SCN5A mutations. Cardiovasc Res 2005; 67:510-519.
37 Clatot J, Ziyadeh-Isleem A, Maugenre S, Denjoy I, Liu H, Dilanian G, Hatem SN, Deschenes I, Coulombe A, Guicheney P, Neyroud N: Dominant-negative effect of SCN5A N-terminal mutations through the interaction of Na(v)1.5 alpha-subunits. Cardiovasc Res 2012; 96:53-63.
38 Hoshi M, Du XX, Shinlapawittayatorn K, Liu H, Chai S, Wan X, Ficker E, Deschenes I: Brugada syndrome disease phenotype explained in apparently benign sodium channel mutations. Circ Cardiovasc Genet 2014;7:123-131.
39 Catterall WA: From ionic currents to molecular mechanisms: the structure and function of voltage-gated sodium channels. Neuron 2000;26:13-25.
40 Frigo G, Rampazzo A, Bauce B, Pilichou K, Beffagna G, Danieli GA, Nava A, Martini B: Homozygous SCN5A mutation in Brugada syndrome with monomorphic ventricular tachycardia and structural heart abnormalities. Europace 2007;9:391-397.